Carbon microsphere anchored g-C_3N_4 for enhanced photocatalytic properties

Qingbo Yu, Kuan Yang and Huiqin Li

Department of Materials Science and Engineering,
Anhui University of Science and Technology,
Huainan, 232001, China
Email: yuqingbo007@163.com
Email: 826245354@qq.com
Email: 1145667468@qq.com
*Corresponding author

Abstract: Graphitic carbon nitride (g-C_3N_4) is a new type of semiconductor material with highly physicochemical stability. In this paper, carbon microsphere anchored g-C_3N_4 composites were prepared by blending g-C_3N_4 with polyvinyl alcohol at high temperature. The structure and morphology of the composites were characterised by X-ray diffraction, infrared spectroscopy, ultraviolet spectroscopy, scanning electron microscopy, and so on. Their properties were tested by electrochemical and photocatalytic experiments. The results show that carbon microspheres can be loaded on the surface of g-C_3N_4 without changing the basic structure of g-C_3N_4 with a proper ration between polyvinyl alcohol and g-C_3N_4. Compared with the pure g-C_3N_4, the photocurrent after modification is increased by 1000 times and the photocatalytic degradation rate is increased by 2.8 times.

Keywords: carbon nitride; polyvinyl alcohol; carbon microsphere; photocatalytic; structure; electrochemical; photocurrent; improvement; semiconductor.

Reference to this paper should be made as follows: Yu, Q., Yang, K. and Li, H. (2021) 'Carbon microsphere anchored g-C_3N_4 for enhanced photocatalytic properties', *Int. J. Nanomanufacturing*, Vol. 17, No. 1, pp.26–36.

Biographical notes: Qingbo Yu is a professor in Anhui University of Science and Technology. He completed her doctoral work at Anhui University. her research interests are in polymer materials and nanocomposites.

Yang Kuan is a postgraduate student in Anhui university of Science and Technology. He mainly engaged in the preparation of materials and the research of photocatalytic degradation.

Huiqin Li is a postgraduate student in Anhui university of Science and Technology. His research interests include nanomaterials, porous materials, biosensors.

Copyright © 2021 Inderscience Enterprises Ltd.

1 Introduction

In recent years, with the rapid development of industrial civilisation, water pollution has gradually threatened human normal production activities (Liu et al., 2016). The traditional treatment methods for water pollution have the disadvantages of energy-extensive consumption, time-consuming, inefficiency. So it is difficult to use on a large scale (Chen et al., 2013). Photocatalysis has gradually come into people's attention due to its economical and effective characteristics. Conventional photocatalysts, such as TiO_2 (Nalid et al., 2017), ZnO (Adnan et al., 2016), ZnS (Han et al., 2017), have low solar utilisation, and are easily corroded to lose photocatalytic activity. Graphitic carbon nitride (g-C_3N_4) with a graphite-like structure, is a metal-free, novel semiconductor photocatalyst with highly response in the visible region (Wang et al., 2009). With the property of excellent electronic band structure and highly physicochemical stability, it have been used in air purification (Takeuchi, 2013; Chen et al., 2019), energy (Zhang et al., 2018; Zhao et al., 2017) and other fields. However, the conventional graphitic carbon nitride (g-C_3N_4) has poor catalytic performance due to poor carrier transport, low reaction site density, and high recombination of electron-hole pairs. In order to compensate for these defects, the catalytic properties are often improved by physical or chemical modification, such as morphology designing (Cui et al., 2018; Ma et al., 2018), element doping (Li et al., 2018; Ran et al., 2015), surface modification (Chan and Yu, 2018), and so on. However, metal or non-metal doping may cause secondary pollution to affect the large-scale use due to the falling off of the dopant. Carbon-based material has structural stability, excellent electrical conductivity and non-biotoxic properties, providing a new way to modify g-C_3N_4. It has been reported that carbon fibre (Ma et al., 2017) and carbon nanotubes (Bai et al., 2018; Xu et al., 2013) can not only increase the absorption of visible light, but also reduce electron-hole recombination, thereby improving photocatalytic performance. However, carbon fibre and carbon nanotubes are difficult to be applied on a large scale due to their complicated preparation procedures and high cost. As an important part of carbon materials, carbon microspheres was widely used due to it can be used as electron transport channels and can be prepared by calcined after simple hydrothermal (Chen et al., 2018; Ding et al., 2018; Zou et al., 2017). Polyvinyl alcohol is a non-toxic and low-cost polymer that can be used as a carbon source by calcination (Fang et al., 2013).

In this paper, carbon microsphere anchored g-C_3N_4 was prepared by calcining after blending polyvinyl alcohol and graphitic carbon nitride (g-C_3N_4). The effect of the ration between polyvinyl alcohol and g-C_3N_4 on the structural properties of the C/g-C_3N_4 was explored.

2 Experimental

2.1 Materials and equipment

Dicyandiamide, methylene blue and polyvinyl alcohol were purchased from Shanghai Jingchun Biochemical Technology Company. XRD measurements were performed using a Philips Shimadzu International's 6000 X-ray diffractometer with Cu radiation from 5 to 60 (2θ) at room temperature in reflection mode. The microstructure of C/g-C_3N_4 composites was studied by scanning electron microscopy (SEM, S-3000N). C/g-C_3N_4

composites were measured by infrared spectroscopy (FT-IR, NICOLET380) in the rage of 500 cm^{-1} to 4000 cm^{-1} with transmission mode. The light absorption of different wavelengths of C/g-C_3N_4 composites was studied by ultraviolet-visible spectrophotometer (UV-2600); The electrical properties of C/g-C_3N_4 composite electrodes were studied by CHI660E electrochemical system (Shanghai Chenhua Instrument Company). Analysis of C/g-C_3N_4 composites using a thermogravimetric testing under nitrogen protection and high temperature difference analyser (SDT2960)

2.2 Preparation of the samples

2.2.1 Preparation of sample 1 (g-C_3N_4)

According to our precious research (Yu et al., 2014), 6 g of dicyandiamide were placed in porcelain boat, and then heated to 550°C for 4 h in N_2 at a heating rate of 2.5°C/min. After the thermal treatment, the porcelain boat was cooled down to room temperature. The yellow sample was collected and milled into powder. Therefore, the pure g-C_3N_4 was obtained and was named CN.

2.2.2 Preparation of sample 2 (carbon/g-C_3N_4 composite)

3 g of polyvinyl alcohol was dissolved in 100 mL of deionised water at 95°C. 0.4 g of CN was placed in 10 mL of deionised water, and was sonicated for 30 min. A certain amount of the configured polyvinyl alcohol solution was added to the CN solution. The mixture was stirred and sonicated for 30 min. Then it was dried at 120°C for 12 h. The dried sample were placed in porcelain boat, and then heated to 550°C for 1.5 h in N_2 at a heating rate of 5°C/min. After cooling down to room temperature, the sample was collected and milled into powder. The obtained products with different the configured polyvinyl alcohol solution weight of 10 mL, 0.25 mL, 0.2 mL and 0.14 mL were denoted as CN-10, CN-0.25, CN-0.2, CN-0.14, respectively.

3 Results and discussion

3.1 Scanning electron microscopy (SEM) analysis

Figure 1 is a SEM image of graphitic carbon nitride (g-C_3N_4) and graphitic carbon nitride (g-C_3N_4) after carbonised with different amounts of polyvinyl alcohol. The strategic choice of PVA is lower thermal-decomposition temperature. It can be clearly found that the pure graphitic carbon nitride (g-C_3N_4) is an aggregate of surface rough layered materials (Figure 1(a)). After carbonised by the addition of polyvinyl alcohol, there was a significant change in the surface of all the catalysts. When the amount of polyvinyl alcohol added is relatively large or small, only the surface of the sample becomes flatter (Figure 1(b)) or a similar hemispherical protrusion is formed on the surface of the sample sheet (Figure 1(d)). When the amount of polyvinyl alcohol is 0.2 mL, microspheres having similar shapes and sizes can be formed on the surface of the sheet (Figure 1(c)).

Figure 1 SEM images of: (a) CN; (b) CN-10; (c) CN-0.2 and (d) CN-0.14

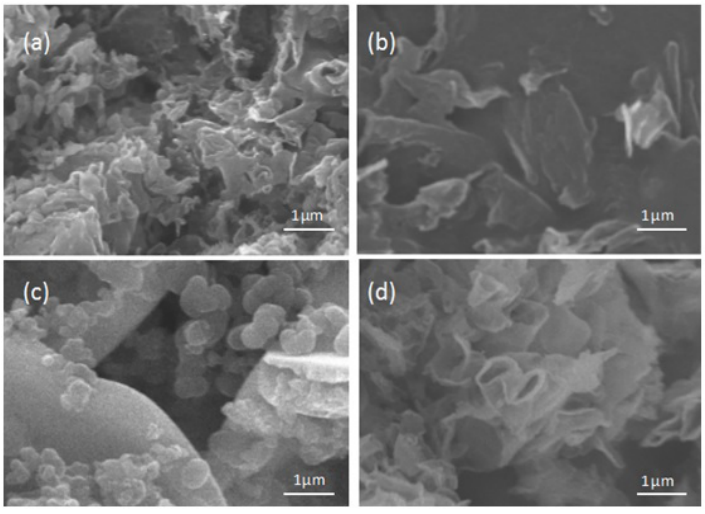

3.2 XRD analysis

The crystal structures of CN, CN-0.14, CN-0.2, CN-0.25 and CN-10 were tested by XRD, and the results are shown in Figure 2. Two typical diffraction peaks at 13.1° and 27.3° were found at the spectra of CN, CN-0.14, CN-0.2 and CN-0.25. The peak at 13.1° corresponds to (100) plane, related to the in-plane structure of tri-s-triazine unites. The peak at 27.3° is indexed to the graphitic carbon nitride (g-C_3N_4) (002) crystal plane which attributed to the conjugated aromatic structure of the interlayer stack (Thomas et al., 2008). It can be seen that the main diffraction peak of the graphitic carbon nitride (g-C_3N_4) modified by a small amount of polyvinyl alcohol carbonisation has not be changed, indicating that the basic crystal structure of the graphitic carbon nitride (g-C_3N_4) remains unchanged. Among them, the decrease of the peak intensity at 13.1° and 27.3° in the spectrum of CN-0.14 and CN-0.25 indicates that the crystallinity decreases. It is due to the partial graphitic carbon nitride (g-C_3N_4) when the carbonisation temperature is raised to 550°C has been decomposed (Cui et al., 2015). CN-0.2 has the highest and the sharpest diffraction peak at 13.1° and 27.3°. The possible reason is that when the temperature increased, part of the graphite carbon nitride decomposed to form 'melon' unit. In the cooling process, since the carbon spheres are similar in structure to the graphitic carbon nitride. And there is an π-π interaction between the carbon spheres and the graphitic carbon nitride. A part of the 'melon' unit grows along the surface of the carbon microspheres, thereby improving its crystallinity (Ma et al., 2017). The spectrum of CN-10 only shows a diffraction peak at 25.4°, which is a typical graphitic carbon (002) crystal plane (Shao et al., 2018). Excessive amount of polyvinyl alcohol were carbonised. And graphitic carbon nitride (g-C_3N_4) sheets were wrapped by the large amount of carbon, which is consistent with the observation of SEM.

Figure 2 (a) XRD patterns of CN, CN-0.14, CN-0.2, CN-0.25 and CN-10 composites (see online version for colours)

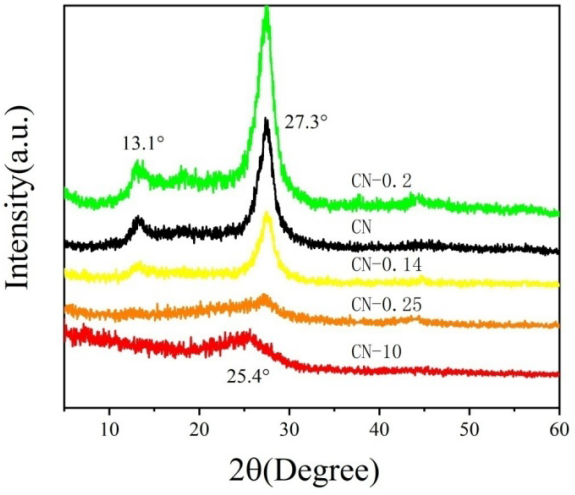

3.3 TG analysis

Figure 3 shows the TG diagram of CN, CN-0.14, and CN-10. It can be clearly found that CN-0.14 and CN-10 remain undecomposed carbon when the temperature reaches 800°C compared to CN. Moreover, as the amount of polyvinyl alcohol increased, the carbon content in the catalyst increased significantly, which is consistent with the SEM observation.

Figure 3 The TG of CN, CN-0.14 and CN-10 composites (see online version for colours)

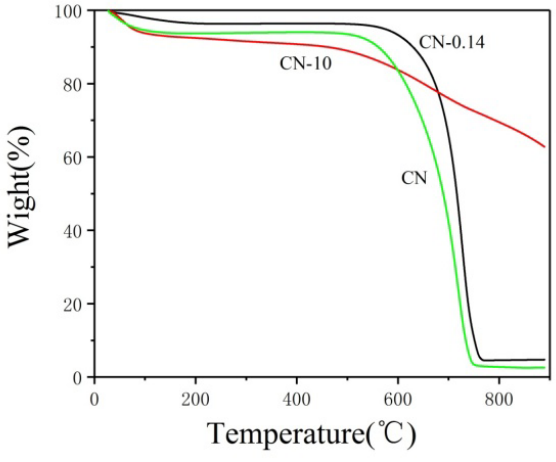

3.4 FT-IR analysis

Figure 4 shows the infrared spectrum of CN, CN-0.14, CN-0.2, CN-0.25 and CN-10. It can be seen from the figure that only the absorption peak of graphitic carbon nitride

(g-C_3N_4) exists, indicating that the catalyst does not contain other impurities and the doping of carbon does not change the basic structure of graphitic carbon nitride (g-C_3N_4). The broad absorption peak at 3000–3700 cm^{-1} may be the OH stretching vibration of the catalyst surface adsorbing moisture or related to N-H in the aromatic group of g-C_3N_4 (Yin et al., 2018). The continuous absorption peak in the middle of 1200–1700 cm^{-1} is the stretching vibration corresponding to C-N and C=N, and the bending vibration absorption peak of the triazine ring structure is located at 810 cm^{-1} (Wang et al., 2018). By comparing the infrared spectra of CN-0.14, CN-0.2, CN-0.25, CN-10 and CN-10, it can be seen that the absorption peak intensity of the infrared spectra of CN-0.14, CN-0.2, CN –0.25 and CN-10 decreased at 1700-1200 cm^{-1}, due to the decomposition of part of the graphitic carbon nitride (g-C_3N_4). With the addition of polyvinyl alcohol too much, the absorption peak of CN-10 at 810 cm^{-1} disappears. It is indicated that too much carbon will coat the graphitic carbon nitride (g-C_3N_4) sheet, which is consistent with the previous analysis. Therefore, it can be inferred that a carbon/graphitic carbon nitride (g-C_3N_4) composite material has been successfully prepared.

Figure 4 FT-IR spectra of CN, CN-0.14, CN-0.2, CN-0.25 and CN-10 composites (see online version for colours)

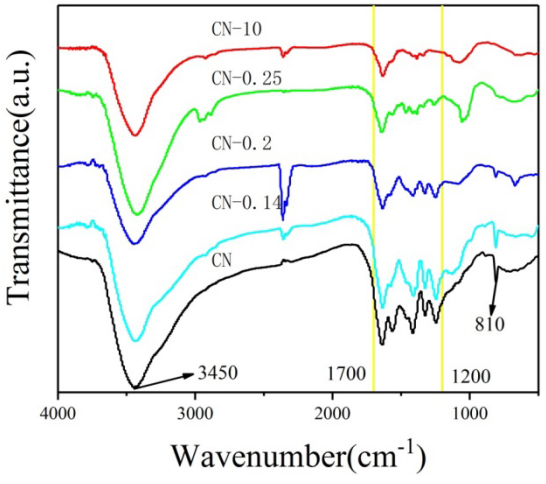

3.5 BET analysis

Figure 5 shows the BET diagram of CN and CN-0.2. The modified graphitic carbon nitride carbon (g-C_3N_4) can be clearly seen from the figure, and its specific surface area is obviously increased. The specific surface area of CN-0.2 increased from 4.61 m^2/g of the pure graphitic carbon nitride carbon (g-C_3N_4) to 74.61 m^2/g, which increased by nearly 18 times.

3.6 UV–Vis spectra analysis

Figure 6 shows the UV-vis spectra of CN, CN-0.14, CN-0.2 and CN-10. It can be seen from the figure that the absorption intensity in the visible region of the modified graphitic carbon nitride (g-C_3N_4) has enhanced relative to graphitic carbon nitride (g-C_3N_4).

Among them, CN-0.2 still has higher absorption intensity at $\lambda = 800$ nm, which may due to increase the specific surface area and increase the absorption of visible light by the formation of carbon microspheres on the surface by calcination (Wang et al., 2018). The absorption curve of CN-10 in the figure is significantly different from others because the graphitic carbon nitride (g-C_3N_4) sheets were wrapped by excessive carbon, which affects the absorption of light by graphitic carbon nitride (g-C_3N_4). This is consistent with the analysis of XRD and SEM.

Figure 5 The BET of CN and CN-0.2 composites

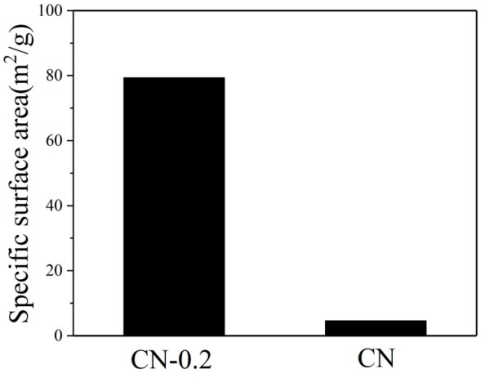

Figure 6 UV–vis diffuse reflectance adsorption spectra of CN, CN-0.14, CN-0.2, CN-0.25 and CN-10 composites (see online version for colours)

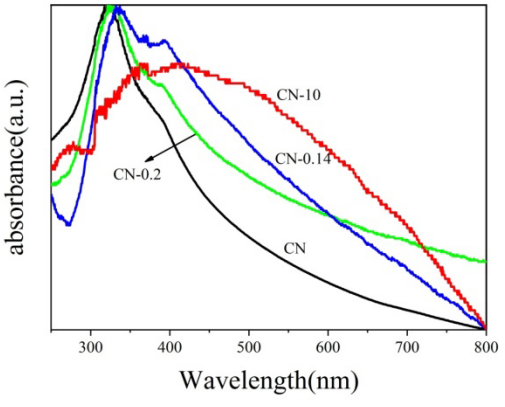

3.7 Electrical performance analysis

Determination of charge transfer resistance of CN and CN-0.2 by electrochemical impedance spectroscopy (EIS). The radius of the circular arc reflected the resistance of the interfacial charge and separation efficiency of the electron–hole pairs, a smaller arc radius of the EIS nyquist plot reflects a higher efficient charge transfer occurring at the

interface. From Figure 7(a)., it can be seen that the semicircle radius of the CN-0.2 curve is smaller than that of CN, indicating that CN-0.2 has superior conductivity. On the one hand, the carbon sphere increases the crystallinity of CN-0.2, and reduces the hydrogen bond formed by the covalent bond at the defect, thereby reducing the additional influence on the excitation carrier (Ou et al., 2017). On the other hand, the carbon microsphere can be used as the interlayer electron passing the bridge, which is beneficial to stimulate the electron transfer to enhance the conductivity (Li et al., 2016). The excitation and transmission efficiency of photogenerated electron-hole under visible light irradiation are further measured by using transient current response. From Figure 7(b), it can be clearly found that the excitation current of CN-0.2 under visible light irradiation is about 1000 times that of CN. Therefore, it can be determined that the carbon microsphere anchored g-C_3N_4 composite prepared by carbonisation of polyvinyl alcohol and graphitic carbon nitride carbon (g-C_3N_4) can effectively improve the photoelectric response of carbon nitride. This is due to the increased specific surface area of CN-0.2 and the enhanced absorption of light, which can excite more electrons and holes and provide more reactive sites for photocatalysis.

Figure 7 (a) Transient photocurrent response under visible light irradiation; (b) electrochemical impedance spectroscopy (EIS) nyquist plots of CN and CN-0.2 composites (see online version for colours)

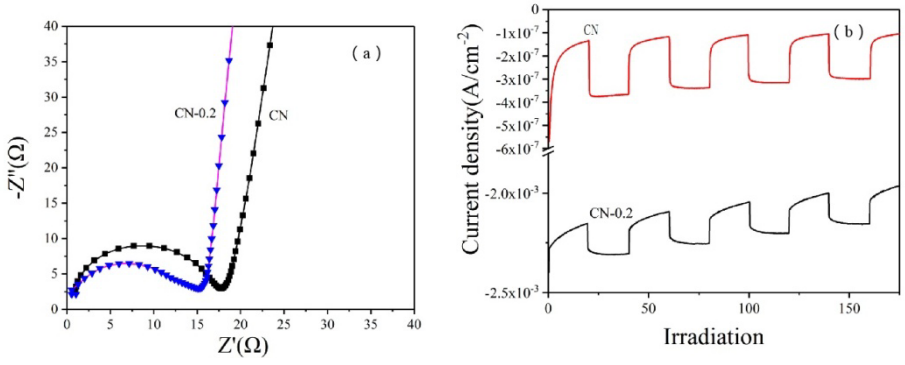

3.8 Evaluation of the photocatalytic activity of the samples

Figure 8 is a photocatalytic diagram of CN, CN-0.14, CN-0.2, CN-0.25 and CN-10. Photocatalytic performance of composite materials as photocatalysts for degradation of methylene blue. According to $InC_0/C = kt$, the degradation rate constant of the prepared sample can be calculated (Table 1). It can be found that the degradation rate of CN-10 is less than that of CN, indicating that the photocatalytic performance was reduced by carbon encasing carbon nitride sheet. Among them, the CN-0.2 degradation rate constant is 2.8 times higher than that of CN. This is attributed to the increase of crystallinity, the reduction of structural defects, the higher absorption of visible light (Chan and Yu, 2018), and the excellent electron transport channels, etc. (Liu et al., 2017), which accelerate the degradation of methylene blue solution.

Figure 8 Comparison of the photocatalytic efficiency of CN, CN-0.14, CN-0.2, CN-0.25 and CN-10 composites under visible light irradiation (see online version for colours)

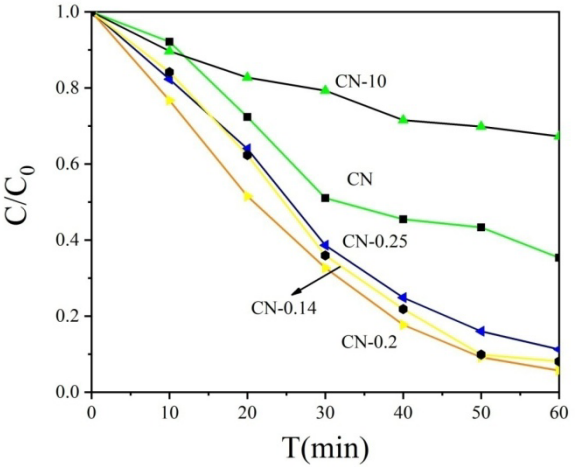

Table 1 Degradation rate of different catalysts

Catalyst	*60 min degradation rate* (%)	*Degradation rate constant k* (min^{-1})
CN	64.65	0.0173
CN-0.14	91.91	0.0419
CN-0.2	94.32	0.0478
CN-0.25	88.75	0.0364
CN-10	32.76	0.00616

4 Conclusion

The carbon/graphitic carbon nitride (g-C_3N_4) composite was successfully prepared by polyvinyl alcohol solution with graphitic carbon nitride (g-C_3N_4) being combined and calcined at high temperature (550°C). The addition of polyvinyl alcohol has great influence on the microstructure and properties of composites. When the addition amount of polyvinyl alcohol is 0.2 mL, carbon microspheres can be formed on the surface of the graphitic carbon nitride (g-C_3N_4) sheet, which is favourable for the crystallisation of graphitic carbon nitride (g-C_3N_4). The specific surface area and the absorption range of visible light are increased, so that the photocatalytic performance and the electrochemical performance can be effectively improved.

References

Adnan, M.A.M., Julkapli, N.M. and Hamid, S.B.A. (2016) 'A review on ZnO hybrid photocatalyst: impact on photocatalytic activities of water pollutant degradation', *Rev Inorg Chem*., Vol. 36, pp.77–104.

Bai, J.X., Han, Q., Cheng, Z.H. and Qu, L.T. (2018) 'Wall-mesoporous graphitic carbon nitride nanotubes for efficient photocatalytic hydrogen evolution', *Chem-Asian J*, Vol. 13, pp.3160–3164.

Chan, D.K.L. and Yu, J.C. (2018) 'Facile synthesis of carbon- and oxygen-rich graphitic carbon nitride with enhanced visible-light photocatalytic activity', *Catalysis Today*, Vol. 310, pp.26–31.

Chen, F.J., Cao, Y.L., Jia, D.Z. and Niu, X.J. (2013) 'Facile synthesis of CdS nanoparticles photocatalyst with high performance', *Ceramics International*, Vol. 39, pp.1511–1517.

Chen, P., Wang, H., Liu, H.J., Ni, Z.L., Li, J.Y., Zhou, Y. and Dong, F. (2019) 'Directional electron delivery and enhanced reactants activation enable efficient photocatalytic air purification on amorphous carbon nitride co-functionalized with O/La', *Appl. Catal B-Environ*., Vol. 242, pp.19–30.

Chen, Y.X., Ji, X.B., Vadivel, S. and Paul, B. (2018) 'Anchoring carbon spheres on BiOBr/g-C3N4 matrix for high-performance visible light photocatalysis', *Ceram Int*., Vol. 44, pp.23320–23323.

Cui, J.G., Qi, D.W. and Wang, X. (2018) 'Research on the techniques of ultrasound-assisted liquid-phase peeling, thermal oxidation peeling and acid-base chemical peeling for ultra-thin graphite carbon nitride nanosheets', *Ultrason Sonochem*., Vol. 48, pp.181–187.

Cui, Y.J., Tang, Y.B. and Wang, X. (2015) 'Template-free synthesis of graphitic carbon nitride hollow spheres for photocatalytic degradation of organic pollutants', *Materials Letters*, Vol. 161, pp.197–200.

Ding, X., Xiao, D., Ji, L., Jin, D., Dai, K., Yang, Z.X., Wang, S.Y. and Chen, H. (2018) 'Simple fabrication of Fe3O4/C/g-C3N4 two-dimensional composite by hydrothermal carbonization approach with enhanced photocatalytic performance under visible light', *Catal Sci Technol.*, Vol. 8, pp.3484–3492.

Fang, W., Cheng, X.Q., Zuo, pp.J., Ma, Y.L. and Yin, G.P. (2013) 'A facile strategy to prepare nano-crystalline Li4Ti5O12/C anode material via polyvinyl alcohol as carbon source for high-rate rechargeable Li-ion batteries', *Electrochim Acta*, Vol. 93, pp.173–178.

Han, Z., Wang, N., Zhang, H. and Yang, X. (2017) 'A Facile hydrothermal route for synthesis of ZnS hollow spheres with photocatalytic degradation of dyes under visible light', *J. Appl Spectrosc*., Vol. 83, pp.1007–1011.

Li, K., Xie, X. and Zhang, W.D. (2016) 'Photocatalysts based on g-C3N4-encapsulating carbon spheres with high visible light activity for photocatalytic hydrogen evolution', *Carbon*, Vol. 110, pp.356–366.

Li, X.W., Chen, D.Y., Li, N.J., Xu, Q.F., Li, H., He, J.H. and Lu, J.M. (2018) 'AgBr-loaded hollow porous carbon nitride with ultrahigh activity as visible light photocatalysts for water remediation', *Appl. Catal B-Environ*., Vol. 229, pp.155–162.

Liu, C.Y., Zhang, Y.H., Dong, F., Reshak, A.H., Ye, L.Q., Pinna, N., Zeng, C., Zhang, T.R. and Huang, H.W. (2017) 'Chlorine intercalation in graphitic carbon nitride for efficient photocatalysis', *Appl Catal B-Environ*., Vol. 203, pp.465–474.

Liu, Y.J., Zhou, F., Zhan, S., Yang, Y.F. and Yin, Y.F. (2016) 'Significantly enhanced performance of g-C3N4/Bi2MoO6 films for photocatalytic degradation of pollutants under visible-light irradiation', *Chem. Res. Chinese U*, Vol. 32, pp.284–290.

Ma, L.N., Wang, G.H., Jiang, C.J., Bao, H.L. and Xu, Q.C. (2018) 'Synthesis of core-shell TiO2@g-C3N4 hollow microspheres for efficient photocatalytic degradation of rhodamine B under visible light', *Applied Surface Science*, Vol. 430, pp.263–272.

Ma, L.T., Fan, H.Q., Fu, K., Lei, S.H., Hu, Q.Z., Huang, H.T. and He, G.P. (2017) 'Protonation of Graphitic Carbon Nitride (g-C3N4) for an Electrostatically Self-Assembling Carbon@g-C3N4 Core Shell Nanostructure toward High Hydrogen Evolution', *ACS Sustain Chem Eng*, Vol. 5, pp.7093–7013.

Ma, T.F., Bai, J. and Li, C.P. (2017) 'Facile synthesis of g-C3N4 wrapping on one-dimensional carbon fiber as a composite photocatalyst to degrade organic pollutants', *Vacuum*, Vol. 145, pp.47–54.

Nalid, N.R., Majid, A., Tahir, M.B., Niaz, N.A. and Khalid, S. (2017) 'Tri-s-triazine-based crystalline carbon nitride nanosheets for an improved hydrogen evolution', *Ceram Int.*, Vol. 43, pp.14552.

Ou, H., Lin, L., Zheng, Y., Yang, pp., Fang, Y. and Wang, X. (2017) 'Tri-s-triazine-based crystalline carbon nitride nanosheets for an improved hydrogen evolution', *Advanced Materials*, Vol.29, No.1700008.

Ran, J.R., Ma, T.Y., Gao, G.P., Du, X.W. and Qiao, S.Z. (2015) 'Porous P-doped graphitic carbon nitride nanosheets for synergistically enhanced visible-light photocatalytic H-2 production', *Energ. Environ. Sci.*, Vol. 8, pp.3708–3711

Shao, B.B., Liu, Z.F., Zeng, G.M., Wu, Z.B., Liu, Y., Cheng, M., Chen, M., Liu, Y.J. and Zhang, W., Feng, H.P. (2018) ' Nitrogen-doped hollow mesoporous carbon spheres modified g-C3N4/Bi2O3 direct dual semiconductor photocatalytic system with enhanced antibiotics degradation under visible light', *Acs Sustain Chem Eng*., Vol. 6, pp.16424–16436.

Taizo, S., Sakiko, T., Kazuhide, K., Tsutomu, H., Yoshiyuki, T., Nobuaki, N. and Koji, T. (2013) 'Activation of graphitic carbon nitride (g-C3N4) by alkaline hydrothermal treatment for photocatalytic NO oxidation in gas phase', *Journal of Materials Chemistry A*, Vol. 1, pp.6489–6496.

Thomas, A., Fischer, A., Goettmann, F., Antonietti, M., Muller, J.O., Schlogl, R. and Carlsson, J.M. (2008) 'Graphitic carbon nitride materials: variation of structure and morphology and their use as metal-free catalysts', J. *Mater Chem*., Vol. 18, pp.4893–4908.

Wang, C., Fan, H.Q., Ren, X.H., Fang, J.W., Ma, J.W. and Zhao, N. (2018) 'Porous graphitic carbon nitride nanosheets by pre-polymerization for enhanced photocatalysis', *Materials Characterization*, Vol. 139, pp.89–99.

Wang, X.C., Maeda, K., Thomas, A., Takanabe, K., Xin, G., Carlsson, J.M., Domen, K. and Antonietti, M. (2009) 'A metal-free polymeric photocatalyst for hydrogen production from water under visible light', *Nat Mater*., Vol. 8, pp.76–80.

Wang, X.Y., Lu, M.Y., Ma, J., Ning, pp. and Che, L. (2018) 'Synthesis of K-doped g-C3N4/carbon microsphere@graphene composite with high surface area for enhanced adsorption and visible photocatalytic degradation of tetracycline', *J. Taiwan Inst Chem E*, Vol. 91, pp.609–622.

Xu, Y., Xu, H., Wang, L., Yan, J., Li, H., Song, Y., Huang, L. and Cai, G. (2013) 'The CNT modified white C3N4 composite photocatalyst with enhanced visible-light response photoactivity', *Dalton Trans*., Vol. 42, pp.7604–7613.

Yin, C.C., Cui, L.F., Pu, T.T., Fang, X.Y., Shi, H.C., Kang, S.F. and Zhang, X.D. (2018) 'Facile fabrication of nano-sized hollow-CdS@g-C3N4 Core-shell spheres for efficient visible-light-driven hydrogen evolution', *Applied Surface Science*., Vol. 456, pp.464–472.

Yu, Q., Li, X. and Zhang, M. (2014) 'One-step fabrication and high photocatalytic activity of porous graphitic carbon nitride synthesised via direct polymerisation of dicyandiamide without templates', *Micro Nano Lett*., Vol. 1, pp.1–5.

Zhang, G., Lin, L., Li, G., Zhang, Y., Savateev, A., Zafeiratos, S., Wang, X. and Antonietti, M. (2018) *Angewandte Chemie*., Vol. 57, No. 9372.

Zhao, S., Zhang, Y.W., Wang, Y.Y., Zhou, Y.M., Qiu, K.B., Zhang, C., Fang, J.S. and Sheng, X.L. (2017) *Journal of Power Sources*, Vol. 370, pp.106.

Zou, Y.J., Shi, J.W., Ma, D.D., Fan, Z.Y., Lu, L. and Niu, C.M. (2017) *Chem Eng J*, Vol. 322, pp.435.